The Wiener Process with a Random Non-Monotone Hazard Rate-Based Drift

Luis Alberto Rodríguez-Picón *[ID], **Luis Carlos Méndez-González** [ID], **Luis Asunción Pérez-Domínguez** [ID] and **Héctor Eduardo Tovanche-Picón** [ID]

Department of Industrial Engineering and Manufacturing, Institute of Engineering and Technology, Universidad Autónoma de Ciudad Juárez, Ciudad Juárez, Chihuahua 32310, Mexico; luis.mendez@uacj.mx (L.C.M.-G.); luis.dominguez@uacj.mx (L.A.P.-D.); hector.tovanche@uacj.mx (H.E.T.-P.)

* Correspondence: luis.picon@uacj.mx

Abstract: Several variations of stochastic processes have been studied in the literature to obtain reliability estimations of products and systems from degradation data. As the degradation trajectories may have different degradation rates, it is necessary to consider alternatives to characterize their individual behavior. Some stochastic processes have a constant drift parameter, which defines the mean rate of the degradation process. However, for some cases, the mean rate must not be considered as constant, which means that the rate varies in the different stages of the degradation process. This poses an opportunity to study alternative strategies that allow to model this variation in the drift. For this, we consider the Hjorth rate, which is a failure rate that can define different shapes depending on the values of its parameters. In this paper, the integration of this hazard rate with the Wiener process is studied to individually identify the degradation rate of multiple degradation trajectories. Random effects are considered in the model to estimate a parameter of the Hjorth rate for every degradation trajectory, which allows us to identify the type of rate. The reliability functions of the proposed model is obtained through numerical integration as the function results in a complex form. The proposed model is illustrated in two case studies based on a crack propagation and infrared LED datasets. It is found that the proposed approach has better performance for the reliability estimation of products based on information criteria.

Keywords: Wiener process; hazard rate; random effects; Hjorth rate

MSC: 62N05; 60H30

1. Introduction

Stochastic modeling is an important strategy that has been applied in diverse scientific areas, specifically to study the evolution of characteristics of interest through time. In some case studies, the behavior's modeling of a certain characteristic may be of interest such that it is possible to predict and measure the performance according to certain predefined indices [1]. A common example is the quality characteristic of a product, for which it is important to model its behavior to be able to ensure that the product will perform its intended function during a certain period. Based on this example, the behavior of a quality characteristic may vary in the life cycle of a product due to aging and the loss of performance, which is the result of the effect of several environmental conditions during the continuous usage. This means that a quality characteristic that is observed during a certain period will behave as decreasing, constant, and increasing. All of these behaviors characterize the life cycle of a product [2,3]. In this sense, the Wiener process (WP) has been presented as an appropriate model to describe these behaviors, due to its important properties and characteristics, such as the fact it allows one to model non-monotone behaviors as it is based on the normal distribution and it is time-indexed [4,5].

In this sense, several modifications of the WP have been proposed in the literature to extend the applicability of the model to other cases where a characteristic of interest has an uncertain evolution through time. Specifically, random effects have been considered for this purpose. For example, Whitmore [6], Pan et al. [7], Wang et al. [8], Zhou et al. [9], Jiang [10], and Xu et al. [11] studied the WP with a random drift under different circumstances to obtain reliability estimations of products. The inclusion of random shocks and competing risk models have also been considered as an alternative to describe the random behaviors of degradation trajectories. For example, Guan et al. [12] proposed a model that considered catastrophic and degradation failures by taking into account the WP and the Weibull distribution, and a Bayesian approach was considered to estimate the parameters of interest. Wang et al. [13] also considered a competing failure approach that integrated the WP and other stochastic processes to model the different stages of the life cycle of a product, and shocks were also integrated in the proposed approach. Zhang et al. [14] proposed a WP with cumulative random shocks that were described by a compound Poisson process; the model was illustrated with the degradation analysis of Li-ion batteries. Zhang et al. [15] considered a class of random shocks named as random abrupt jumps that defined multiple phases of a degradation trajectory; they considered a WP as the base of the model and proposed an estimation scheme to obtain the first-hitting time distribution of the degradation process. In this sense, Sun et al. [16] also developed a model based on the WP, and random shocks that were described by a Poisson process, but they also considered a nonlinear version of the WP; this was achieved by considered a time transformation in the modeling.

Nonlinear versions of the WP have also been considered in the literature to develop new approaches to deal with the randomness of degradation trajectories. Palayangoda et al. [17], Liu et al. [18], Lin et al. [19], Wang et al. [20], and Lyu et al. [21] considered accelerated degradation tests to propose nonlinear versions of the WP to characterize reliability functions, remaining useful life functions, or optimal burn-in policies for different applications. Other transformations of the WP have also been proposed. For example, Giorgio and Pulcini [22] and Giorgio et al. [23] proposed a WP that took into account that the degradation increments are not necessarily positive and that each increment depends on the current degradation level; they proposed a Bayesian approach to estimate the parameters of that model. Muhammad et al. [24] studied a similar approach where non-negative increments were considered; they developed this approach by letting the rate of the process be described by a transmuted–truncated normal distribution. On the other hand, a phenomenon of interest such as the relaxation effects in lithium-ion batteries has led to interesting modeling approaches to obtain reliability estimations. This case was studied by Xu et al. [25] and Xu et al. [26], where they considered a WP to obtain the remaining useful life prediction and state-of-health estimation of batteries.

An interesting approach that has been studied lately relies on integrating hazard rate functions in the parametrization of the WP. Hazard rate functions are important functions that define the conditional probability of failure given the reliability at certain time, it can also be interpreted as a rate of failures for a certain period. This function defines the three stages of the life cycle of a product, infant mortality (increasing rate), useful life (constant rate), and wear-out (increasing rate), where all three stages form a bathtub shape. In this sense, multiple probability distribution functions (PDFs) have been proposed in the literature with the aim of obtaining a hazard rate that can identify all three stages. These functions are of interest, as when they are integrated in a stochastic process, it is possible to identify whether a degradation trajectory is increasing, constant, decreasing, or if it has a bathtub shape. Peng et al. [27] considered this approach for the inverse Gaussian process, where the hazard rate of the Weibull distribution was considered as the drift parameter of the process. Rodríguez-Picón et al. [28] also considered the inverse Gaussian process but extended the approach by considering six hazard rate functions, such as the Lai modified Weibull, Xie modified Weibull, Schabe, Chen, and Dimitrakopoulu, in the drift parameter of the process to analyze the degradation process of two case studies. They also

considered random effects in the multiple models to account for unit-to-unit variation with the objective of identifying the type of degradation trajectory. Moreover, Giorgio et al. [29] proposed a WP with a drift parameter based on the Weibull hazard rate; they obtained the reliability and remaining useful life functions and considered random effects in the scale parameter of the Weibull rate, which did not allow them to individually characterize the trajectories.

The previously discussed works provide different approaches to model degradation trajectories under different circumstances. However, further extensions are needed. In this paper, we provide a modeling approach based on the WP that considers a hazard rate function as the drift parameter. Furthermore, random effects are considered in the model with the objective of characterizing the behavior of each degradation trajectory. For example, in the case of the Weibull hazard rate, the shape parameter (β) defines the behavior of the rate, i.e., if $\beta < 1$ the rate is decreasing, if $\beta = 1$, it is constant, and if $\beta > 1$, it is increasing. Then, if the Weibull hazard rate is defined as the drift in the WP and it is assumed that β is random for every trajectory, it is possible to characterize the behavior of the degradation trajectories individually when estimating β. For this reason, we consider the Hjorth hazard rate, as this rate allows us to characterize the same behaviors of the Weibull rate but also including a bathtub behavior and the increasing rate can be characterized as constantly increasing or exponentially increasing [30], which extends the possible characterizations. Individual characterizations of trajectories are an important aspect, since increasing trajectories will reach a critical level in much less time in comparison with decreasing behaviors, which at the end is reflected in the reliability estimation of a product.

The rest of the paper is organized as follows: In Section 2, we provide the proposed modeling approach based on the WP and the Hjorth hazard rate, the PDF of the stochastic process with random effects is presented, and the reliability function is provided. In Section 3, we discuss the details about the scheme to estimate the parameters, and the estimation of the WP with a random hazard rate is implemented based on a Bayesian approach by considering the Gibbs sampler in the OpenBUGS 3.2.3 software. The method to obtain the reliability function is also described, and a numerical integration is considered because that function results in a complex form. In Section 4, we illustrate the proposed approach by implementing the model in two case studies based on a crack propagation and a infrared light emitting diode (IRLED) datasets. Finally, in Section 5, we provide the conclusions of the manuscript and insights for future research.

2. The Wiener Process with Hazard Rate Functions

In this section, we describe the considered models and how they are integrated for the proposed approach. First, we discuss the WP, which is a non-monotone stochastic process describing the behavior of a random variable $X(t)$ at times $t \geq 0$, which can be defined as

$$X(t) = X(0) + \mu(t) + \sigma B(t), \tag{1}$$

where μ is the drift parameter of the process, also known as the degradation rate, σ is the diffusion parameter, and $B(t)$ is the standard Brownian motion. $X(0)$ represents the initial level of the process at $t = 0$; in this paper, we assumed that $X(0) = 0$. In general, the increments $\Delta X(t) = X(t + \Delta t) - X(t)$ of the WP are independent and follow a normal distribution with a PDF defined as $f(\Delta X(t)|\mu, \sigma)$ and described by

$$f(\Delta X(t)|\mu, \sigma) = \frac{1}{\sqrt{2\pi\Delta t}\sigma} exp - \left\{ \frac{(\Delta X(t) - \mu\Delta t)^2}{2\sigma^2\Delta t} \right\}. \tag{2}$$

By considering that a degradation test has been performed for $i = 1, 2, \ldots, n$ specimens and that degradation measurements have been observed at times t_i for $j = 1, 2, \ldots, m$ inspection times, then the increments $\Delta X_i(t_j) = X_i(t_j) - X_i(t_j - 1)$ follow a normal distribution as $\Delta X_i(t_j) \sim f(\mu\Delta t_j, \sigma^2\Delta t_j)$, where $\Delta t_j = t_j - t_{j-1}$. As previously discussed, μ is

considered as a rate function of the process that can be characterized in different forms. In this paper, we considered one hazard rate defined as

$$h(t) = \delta t + \frac{\theta}{1 + \beta t}. \tag{3}$$

The function in (3) is the Hjorth hazard rate, where δ is the location parameter, β is a scale parameter, and θ represents a shape parameter [30]. This rate has important characteristics that are illustrated in Figure 1. As a comparison, we also provide an illustration of the Weibull rates to demonstrate that more behaviors can be characterized with the Hjorth rate.
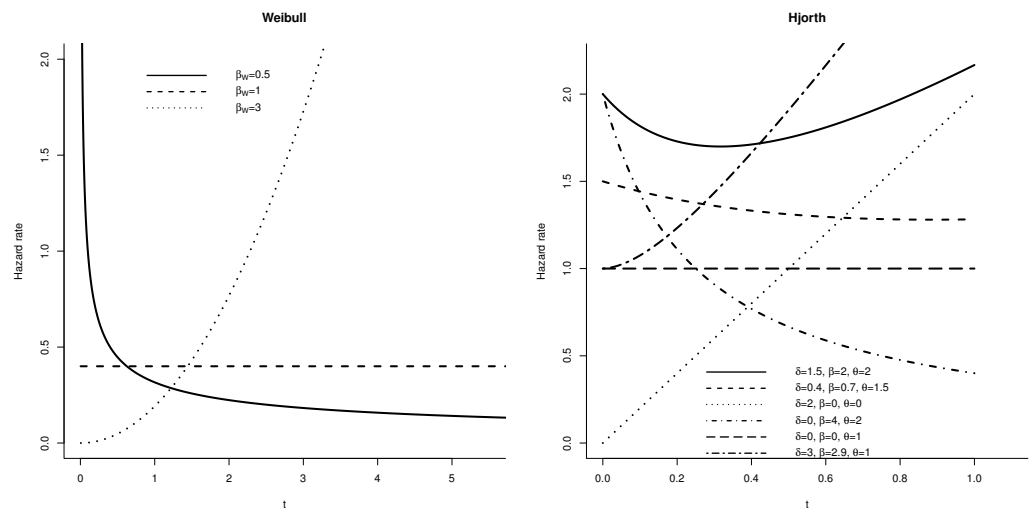

Figure 1. Illustrations of the Weibull and Hjorth hazard rates under different variations of parameters.

In the case of the Hjorth rate, the rate is increasing when $\delta > \theta \beta$. Specifically, it has a constant increasing behavior when θ and β are 0 and $\delta > 0$, and it is exponentially increasing when $\delta > \theta \beta$ but $\theta \beta \approx \delta$. It is decreasing when $\delta = 0$, and it is constant when δ and β are 0. Finally, it has a bathtub shape when $0 < \delta < \theta \beta$. As can be noted, the Hjorth rate has more flexibility to adapt more behaviors including the ones described by the Weibull rate. For this reason, in this paper we propose to consider this hazard rate as the drift function of the WP; thus,

$$\mu_h(t) = h(t). \tag{4}$$

which defines the fact that $\Delta X_i(t_j)$ follows a PDF $f(\mu_h \Delta t_j, \sigma^2 \Delta t_j)$. Indeed, this approach allows a certain flexibility in the stochastic process to obtain a generalized characterization of the behavior of the degradation trajectories. However, an individual characterization is more convenient for the modeling of multiple trajectories. Thus, random effects were considered for unit-to-unit heterogeneity, i.e., one parameter of the hazard rate function was random among the multiple trajectories, which meant that it was estimated individually for each trajectory. This allowed us to individually define the rate of each trajectory as constant, increasing, decreasing, or following a bathtub shape.

In the case of the WP with a Hjorth rate, δ_i is described by a gamma distribution $f(a_H, b_H)$, where a_H represents the shape parameter, and b_H represents the scale parameter. δ_i was assumed to introduce the random effects as this parameter defines the shape of the rate for this distribution. By considering (2), the PDFs of the WP with a random hazard rate based drift were defined as

$$f(\Delta X_i(t_j)|a_H, b_H, \theta, \beta, \sigma) = \int_0^\infty f(\Delta X_i(t_j)|\delta_i, \theta, \beta, \sigma) \times f(\delta_i|a_H, b_H)d\delta. \tag{5}$$

On the other hand, an important aspect of interest in degradation modeling is related to the moment of failure of a degrading product of interest. This moment occurs when the degradation accumulates to a certain level, which is defined as a critical level ω at which the product does not meet the required performance, which defines a soft failure. This moment is defined as a first-hitting time $t_\omega = inf\{X_i(t_j) \geq \omega\}$. It is known that the first-hitting time distribution of the WP results is an inverse Gaussian distribution (IGD), as the mean and shape parameters are $\omega/\hat{\mu}$ and $\omega^2/\hat{\sigma}^2$, respectively [12]. Thus, the reliability function was defined as

$$R(t_\omega|\hat{\mu}, \hat{\sigma}) = 1 - \left[\Phi\left[\frac{1}{\hat{\sigma}}\sqrt{\frac{1}{t_\omega}}(\hat{\mu}t_\omega - \omega) \right] + exp\left\{ \frac{2\hat{\mu}\omega}{\hat{\sigma}^2} \right\} \times \Phi\left[-\frac{1}{\hat{\sigma}}\sqrt{\frac{1}{t_\omega}}(\hat{\mu}t_\omega - \omega) \right] \right].$$

By considering (4) for the Hjorth rate, and that δ_i is a random parameter, then the reliability function for the proposed model is

$$R_H\left(t_\omega|\hat{a}_H, \hat{b}_H, \hat{\theta}, \hat{\beta}, \hat{\sigma} \right) = \int_0^\infty R\left(t_\omega|\delta_i, \hat{\theta}, \hat{\beta}, \hat{\sigma} \right) \times f\left(\delta_i|\hat{a}_H, \hat{b}_H \right) d\delta. \qquad (6)$$

The parameters $\left(\hat{a}_H, \hat{b}_H, \hat{\theta}, \hat{\beta}, \hat{\sigma} \right)$ are required to be previously estimated from (5) to obtain the reliability function from the proposed approach.

3. The Estimation of Parameters

In this section, we discuss the estimation of the parameters of the proposed modeling approach. We first discuss the estimation of the WP–Hjorth model defined in (5). As can be noted, this model results in a complex form, as random effects are included in terms of (δ_i). For this, we considered a Bayesian approach to obtain the estimations of $\left(\hat{a}_H, \hat{b}_H, \hat{\theta}, \hat{\beta}, \hat{\sigma} \right)$. We used the OpenBUGS software for this purpose, as it integrates the Markov chain Monte Carlo (MCMC) and the Gibbs sampler. These methods allow the estimation of complex joint densities that require complex integration. Indeed the main application of MCMC and Gibbs sampler is within the context of Bayesian estimation, as the posterior distributions under this estimation scheme is a joint function of a likelihood function and some prior distributions that require integration.

In the first instance, for all the parameters of interest $(a_H, b_H, \theta, \beta, \sigma)$, we defined non-informative prior gamma distributions as $\theta \sim f(a_\theta, b_\theta)$, $\beta \sim f(a_\beta, b_\beta)$, $\sigma \sim f(a_\sigma, b_{\sigma_\prime})$, where in all cases, a represents the shape parameter, and b represents the scale parameter. As δ_i was considered to be random with gamma PDF $f(a_H, b_H)$, then non-informative gamma prior distributions were also assumed to be $a_H \sim f(c_a, d_a)$ and $b_H \sim f(c_b, d_b)$. Then, by considering that $i = 1, 2, \ldots, n$ degradation increments were observed for $j = 1, 2, \ldots, m$ inspections, the likelihood distribution from (5) was defined as

$$L\left(\Delta X_i(t_j)|a_H, b_H, \theta, \beta, \sigma \right) = \prod_{i=1}^{n}\left\{ f(\delta_i|a_H, b_H) \prod_{j=1}^{m} f\left(\Delta X_i(t_j)|\delta_i, \theta, \beta, \sigma \right) \right\}. \qquad (7)$$

By considering this likelihood function and the previously discussed prior distributions, then the posterior distribution became

$$p\left(a_H, b_H, \theta, \beta, \sigma|\Delta X_i(t_j) \right) = L\left(\Delta X_i(t_j)|a_H, b_H, \theta, \beta, \sigma \right) \times f(a_H) \times f(b_H) \times f(\theta)$$
$$\times f(\beta) \times f(\sigma). \qquad (8)$$

The MCMC–Gibbs sampler was implemented in openBUGS to sample the posterior function in (8) to obtain the estimations $\left(\hat{a}_H, \hat{b}_H, \hat{\theta}, \hat{\beta}, \hat{\sigma} \right)$. For all cases, a total of 180,000 iterations were considered to define the estimation of the parameters of interest, and 20,000 iterations were considered for burn-in purposes.

Once these estimations were obtained, it was possible to assess the reliability by considering the reliability function in (6). It can be noted that the reliability should be obtained by solving this complex integral. In this paper, we characterized the reliability by numerically solving (6) using the R 4.3.2 software and the estimated parameters $\left(\hat{a}_H, \hat{b}_H, \hat{\theta}, \hat{\beta}, \hat{\sigma}\right)$. The programming of this integral was as follows,

```
integrand <- function (t,δᵢ) {
f₁ <- SuppDists::pinvGauss(t_ω,ω/(δᵢt + (θ̂/(1 + β̂t))),ω²/σ̂²)
f₂ <- dgamma(δᵢ,âₕ,b̂ₕ)
return (f1 * f2)
}

cdf=sapply( seq(0.000001,2,0.01),
function(t) integrate(integrand,lower=0,upper=Inf,t=t)$value)
```

The first part of the code represents the integrand which consists in the multiplication of the reliability function in $R_H\left(t_\omega | \delta_i, \hat{\theta}, \hat{\beta}, \hat{\sigma}\right)$ in (6) and the PDF of the random effects parameter $f\left(\delta_i | \hat{a}_H, \hat{b}_H\right)$. Note that the mean parameter of the IGD in f_1 is defined as $\omega/(\delta_i t + (\hat{\theta}/(1 + \hat{\beta}t)))$, according to (4). Then, the integral is numerically solved by using the *sapply* and the *integrate* functions in *cdf* at the end of the code.

4. Implementation of the Proposed Approach

To illustrate the proposed model, we first considered the crack propagation dataset from Wu and Ni [31]. This dataset was obtained from an experimental study which was performed to obtain fatigue crack growth data from a batch of 2024-T351 aluminum alloy plate specimens that are used in aircrafts. The crack propagation trajectories for 30 specimens are presented in Figure 2.

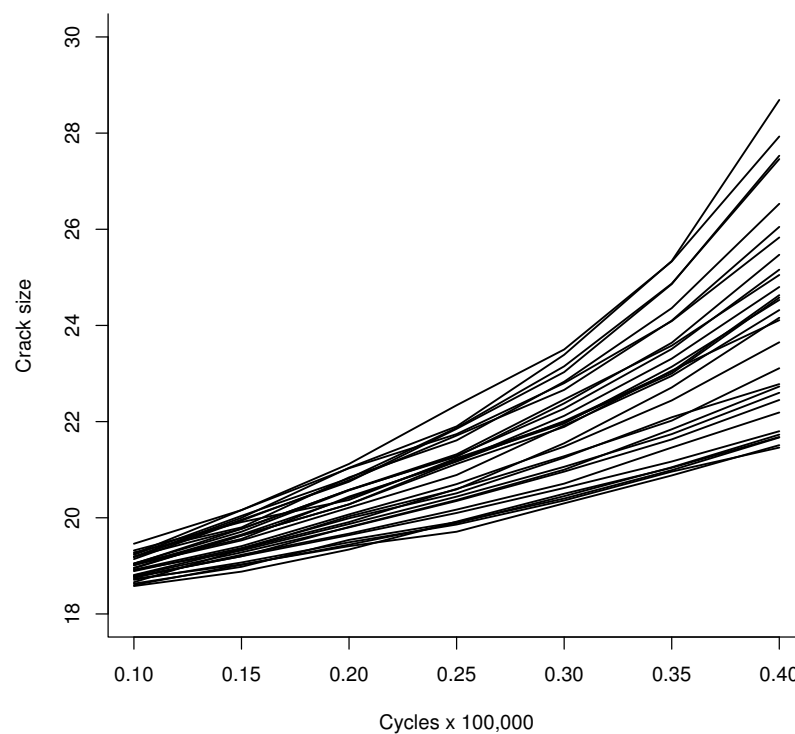**Figure 2.** Crack propagation trajectories for 30 2024-T351 aluminum alloy plate specimens.

The WP was assumed to model the crack propagation trajectories by considering a Hjorth rate with random effects. For this, we considered the model in (5) and estimated the parameters $\left(\hat{a}_H, \hat{b}_H, \hat{\theta}, \hat{\beta}, \hat{\sigma}\right)$ based on a Bayesian approach. The previously discussed prior

distributions for every parameter and the likelihood function in (7) were assumed, and the posterior distribution in (8) was sampled via MCMC–Gibbs sampling in the OpenBUGS software. The obtained estimations are provided in Table 1, where the mean estimations for every parameter are provided in the second column, along with the standard deviation (sd), Monte Carlo (MC) error, and the percentiles at 2.5%, 50%, and 97.5%. It should be noted that in all the parameters, the MC error is less than 5% of the standard deviation of the error, which implies that convergence was achieved for the estimation of all the parameters.

Table 1. Obtained estimations for the WP–Hjorth random effects model.

|	Mean	sd	MC Error	$p_{0.025}$	$p_{0.5}$	$p_{0.975}$
β	0.06331	0.009791	4.43×10^{-4}	0.04751	0.06209	0.08777
b_H	25.6	8.619	0.3817	13	24.25	46.61
a_H	188.1	69.15	3.12	90.45	176.6	360.7
σ	7.092	0.8213	0.005439	5.575	7.061	8.779
θ	120.2	25	1.204	70.88	116.2	173.7
δ_1	6.704	0.6512	0.03045	5.368	6.642	8.035
δ_2	6.935	0.6517	0.03047	5.594	6.871	8.258
δ_3	7.688	0.6559	0.03063	6.336	7.625	9.024
δ_4	7.784	0.6559	0.03062	6.429	7.722	9.12
δ_5	7.479	0.6549	0.0306	6.135	7.416	8.817
δ_6	7.381	0.6535	0.03053	6.032	7.321	8.706
δ_7	7.882	0.6566	0.03064	6.529	7.822	9.213
δ_8	6.679	0.6503	0.03039	5.345	6.616	8.004
δ_9	8.241	0.6594	0.03074	6.886	8.182	9.575
δ_{10}	6.608	0.6499	0.03038	5.27	6.545	7.935
δ_{11}	6.849	0.6507	0.03042	5.514	6.784	8.175
δ_{12}	8.206	0.6579	0.0307	6.856	8.146	9.541
δ_{13}	7.376	0.6539	0.03054	6.027	7.315	8.706
δ_{14}	7.306	0.6546	0.03059	5.957	7.245	8.639
δ_{15}	6.696	0.6507	0.03042	5.362	6.634	8.017
δ_{16}	7.552	0.6553	0.03061	6.2	7.49	8.885
δ_{17}	7.399	0.6542	0.03057	6.052	7.336	8.73
δ_{18}	7.278	0.6538	0.03055	5.937	7.215	8.611
δ_{19}	6.917	0.6526	0.03051	5.573	6.853	8.245
δ_{20}	6.598	0.6505	0.03042	5.267	6.536	7.929
δ_{21}	7.318	0.6538	0.03055	5.974	7.256	8.65
δ_{22}	6.677	0.6511	0.03044	5.344	6.614	8.005
δ_{23}	7.155	0.6527	0.03051	5.816	7.093	8.479
δ_{24}	6.791	0.6513	0.03043	5.457	6.728	8.118
δ_{25}	7.475	0.6541	0.03056	6.123	7.411	8.806
δ_{26}	8.169	0.6569	0.03064	6.819	8.11	9.506
δ_{27}	7.033	0.6534	0.03053	5.691	6.972	8.367
δ_{28}	6.861	0.6517	0.03047	5.514	6.801	8.184
δ_{29}	7.644	0.6545	0.03058	6.292	7.583	8.972
δ_{30}	8.546	0.6603	0.03078	7.187	8.489	9.877

It was previously discussed that random effects for the proposed model were taken into account to individually characterize the degradation trajectories. In this case, the parameter δ_i of the Hjorth rate was assumed as random to account for this individual characterization. As can be noted from Table 1, an estimation of δ_i, $i = 1, 2, \ldots, 30$ was obtained for every crack propagation trajectory. Then, it was possible to identify the type of rate for every trajectory by considering the individual estimations of $\hat{\delta}_i$ and $\hat{\theta}, \hat{\beta}$. The degradation rate is increasing when $\hat{\delta}_i > \hat{\theta}\hat{\beta}$, it has a bathtub shape when $0 < \hat{\delta}_i < \hat{\theta}\hat{\beta}$, and it is decreasing when $\hat{\delta}_i = 0$. In the first instance, none of the trajectories were decreasing, as can be noted in Figure 2; this is well identified as none of the $\hat{\delta}_i$ in Table 1 are zero and their $p_{0.025} > 0$. Furthermore, none of the trajectories were constant through t, as neither $\hat{\delta}_i$ nor $\hat{\beta}$ were zero, and for $\hat{\beta}$, its $p_{0.025} > 0$. In Table 2, we provide the individual identification for

the 30 crack propagation trajectories by considering the previously discussed rules and the estimated parameters in Table 1.

Table 2. Identification of the degradation rates for the crack propagation trajectories.

Trajectory (i)	$\hat{\delta}_i$	$\hat{\theta}\hat{\beta}$	Rate Shape
1	6.704	7.609862	Bathtub
2	6.935	7.609862	Bathtub
3	7.688	7.609862	Increasing
4	7.784	7.609862	Increasing
5	7.479	7.609862	Bathtub
6	7.381	7.609862	Bathtub
7	7.882	7.609862	Increasing
8	6.679	7.609862	Bathtub
9	8.241	7.609862	Increasing
10	6.608	7.609862	Bathtub
11	6.849	7.609862	Bathtub
12	8.206	7.609862	Increasing
13	7.376	7.609862	Bathtub
14	7.306	7.609862	Bathtub
15	6.696	7.609862	Bathtub
16	7.552	7.609862	Bathtub
17	7.399	7.609862	Bathtub
18	7.278	7.609862	Bathtub
19	6.917	7.609862	Bathtub
20	6.598	7.609862	Bathtub
21	7.318	7.609862	Bathtub
22	6.677	7.609862	Bathtub
23	7.155	7.609862	Bathtub
24	6.791	7.609862	Bathtub
25	7.475	7.609862	Bathtub
26	8.169	7.609862	Increasing
27	7.033	7.609862	Bathtub
28	6.861	7.609862	Bathtub
29	7.644	7.609862	Increasing
30	8.546	7.609862	Increasing

From Table 2, it can be noted that trajectories $(3, 4, 7, 9, 12, 26, 29, 30)$ were identified as having an increasing degradation rate, while trajectories $(1, 2, 5, 6, 8, 10, 11, 13, 14, 15, 16, 17, 18, 19, 20, 21, 22, 23, 24, 25, 27, 28)$ were identified as having a bathtub shape rate. In Figure 3, a graphical illustration of the characterization for every trajectory is provided under two schemes. Specifically, in Figure 3a, we provide the identification for every crack propagation trajectory based on Figure 1; it can be noted that the increasing rate trajectories are identified at the top of the figure and are marked with dashed red lines. The trajectories with a bathtub rate are identified with solid black lines. It should be noted that when $\hat{\delta}_i > \hat{\theta}\hat{\beta}$, i.e., when increasing rates are identified, $\hat{\theta}\hat{\beta} \approx \hat{\delta}_i$, which means that the crack propagation trajectories have an exponentially increasing rate, as can be noted in the behaviors of these trajectories in Figure 3a. On the other hand, in Figure 3b, an illustration of the Hjorth rate based on the estimations from Table 1 and the rate in (3) is provided. From this figure, it can be noted that the rates marked in dashed red lines are exponentially increasing as the similarly identified crack propagation rates in Figure 3a, while the solid black lines have a bathtub shape rate according to the identified crack propagation trajectories in Figure 3a.

Trajectories

(**a**)
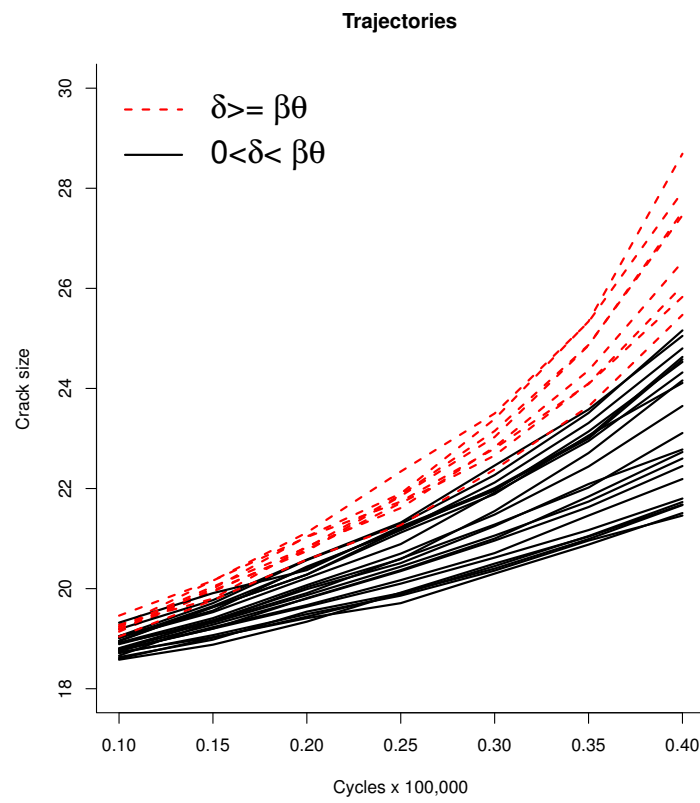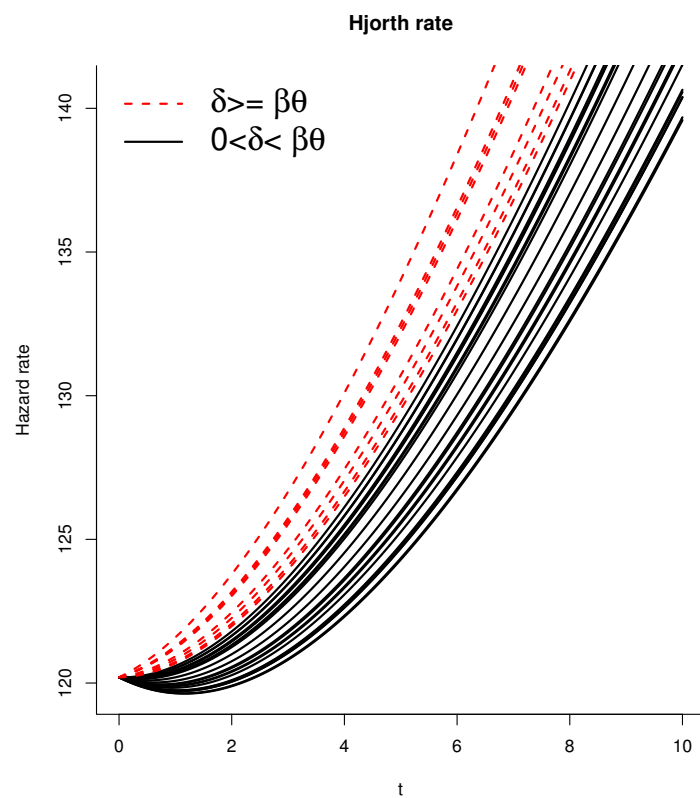
Hjorth rate

(**b**)

Figure 3. Characterization of the crack propagation trajectories and the Hjorth rates. (**a**) Identification of the crack propagation trajectories. (**b**) Illustration of the Hjorth rate for the estimated values of $\hat{\delta}_i$.

Once the characterization of the crack propagation trajectories was defined, it was necessary to estimate the reliability of the product. For this, we considered the reliability function in (6) and the estimated parameters in Table 1. In this case, a value of $\omega = 50$ was considered to establish the critical level of degradation at which a failure of the product occurred. Then, the integral for this function was numerically solved by considering the code provided at the end of Section 3. The estimated reliability for the WP–Hjorth model with random effects is presented in Figure 4 as a solid black line. As a comparison, we also estimated the reliability of the constant-drift WP (CDWP) $R(t_\omega | \hat{\mu}, \hat{\sigma})$ which can be obtained as indicated at the end of Section 2. The estimated parameters for the CDWP were $\hat{\mu} = 1.748$ and $\hat{\sigma} = 2.256$. This reliability function is presented in Figure 4 as a dashed black line. It can be noted that the CDWP overestimated the reliability from $t = 0$ to approximately $t = 30$, then the reliability tended to be lower for $t > 30$ in comparison with the reliability form the WP–Hjorth model.

To further assess the fitting of the proposed model, we also considered the deviance information criterion (DIC) to compare the performance of both models. The DIC is defined as $DIC = -2log\big(L(\Delta X_i(t_j)|\phi)\big) + 2p_{DIC}$, where ϕ is a vector of parameters of interest, in this case $\phi = \left(\hat{a}_H, \hat{b}_H, \hat{\theta}, \hat{\beta}, \hat{\sigma}\right)$ for the W–Hjorth model, and p_{DIC} is an estimate of the effective number of parameters obtained as $\bar{D}(\Delta X_i(t_j)|\hat{\phi}) - D(\Delta X_i(t_j)|\hat{\phi}) = E\big(-2log\big(L(\Delta X_i(t_j)|\phi)\big)|X_i(t_j)\big) - 2log\big(L(\Delta X_i(t_j)|\phi)\big)$. The likelihood function for the WP–Hjorth model with random effects is provided in (7), while the likelihood of the CDWP model can be obtained with

$$L\big(\Delta X_i(t_j)|\mu, \sigma\big) = \prod_{i=1}^{n} \prod_{j=1}^{m} \big\{ f\big(\Delta X_i(t_j)|\mu, \sigma\big) \big\}.$$

The estimated DIC values were $DIC = 44.95$ for the WP–Hjorth model with random effects and $DIC = 244.4$ for the CDWP model. It is known that the model that has the lowest DIC value is considered to be the best fitting model [32]. In this case, the proposed model resulted in the lowest DIC value which confirmed the best fitting model was the one that individually characterized the crack propagation trajectories.
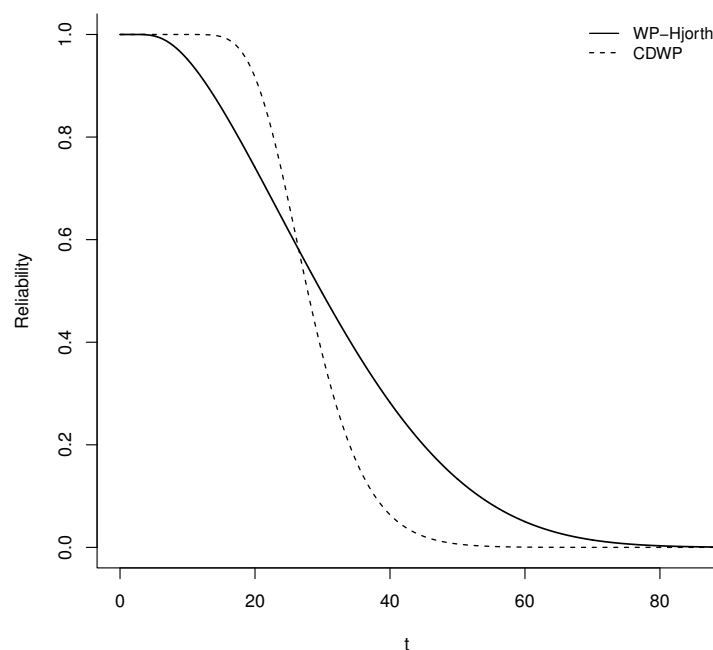

Figure 4. Reliability functions for the WP–Hjorth model with random effects and the CDWP.

Implementation in a IRLED Dataset

To further illustrate the proposed approach, we also considered the IRLED dataset from Yang [33]. These degradation data consist in measurements of the variation ratio of the luminous power of 15 specimens. A degradation test was performed under 320 mA to accelerate the degradation of the performance characteristic. The degradation trajectories are illustrated in Figure 5.
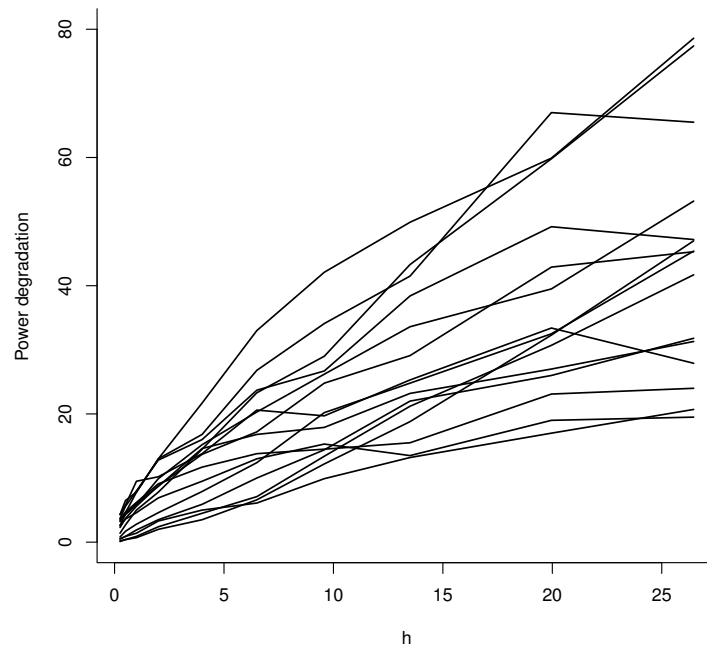

Figure 5. Degradation trajectories from the IRLED dataset.

As in the previous case study, the WP with a Hjorth rate was considered to fit the degradation dataset. A Bayesian approach was also considered to sample (8) via MCMC–Gibbs sampling in OpenBUGS by considering the iterations discussed in Section 3. The obtained estimations are provided in Table 3 in the mean column. Furthermore, the sd, MC error, and some percentiles are also provided. It can be noted that 15 estimations for $\hat{\delta}_i$ were obtained, which means that the degradation rate for every trajectory could be individually characterized. In this sense, in Table 4, we provide a comparison or every estimated $\hat{\delta}_i$ with $\hat{\theta}\hat{\beta}$. From this table, it can be noted that the trajectories $(1, 2, 3, 4, 5, 6, 7, 11, 12, 13, 14, 15)$ were identified as having a bathtub shape, as $0 < \hat{\delta}_i < \hat{\theta}\hat{\beta}$, while trajectories $(8, 9, 10)$ were identified as having an increasing degradation rate, as $\hat{\delta}_i > \hat{\theta}\hat{\beta}$. These behaviors can be better visualized in Figure 6, where the degradation trajectories that were identified as having an increasing rate are presented as red dashed lines, and are on top of the other trajectories, which means that these trajectories indeed had a larger degradation rate, related to the identified increasing behavior. It can also be noted that the other trajectories that were identified to have a bathtub shape are presented as black continuous lines. It can be easily concluded that trajectories have a lower degradation rate, which relates to the individual identification of their degradation rate.

Table 3. Parameter estimations of a WP with a Hjorth rate on the IRLED dataset.

	Mean	**sd**	**MC Error**	$p_{0.025}$	$p_{0.5}$	$p_{0.975}$
β	15.69	30.88	1.307	0.001209	2.272	111.2
δ_1	1.19	0.2769	0.005838	0.6514	1.19	1.728
δ_2	1.132	0.279	0.006521	0.591	1.129	1.676
δ_3	1.076	0.279	0.007097	0.5403	1.074	1.625
δ_4	1.556	0.2803	0.001381	1.016	1.551	2.127

Table 3. *Cont.*

	Mean	sd	MC Error	$p_{0.025}$	$p_{0.5}$	$p_{0.975}$
δ_5	1.603	0.2821	0.001205	1.056	1.596	2.175
δ_6	1.758	0.2942	0.002153	1.201	1.748	2.358
δ_7	1.629	0.2835	0.001187	1.085	1.624	2.205
δ_8	2.414	0.3776	0.01026	1.665	2.419	3.144
δ_9	2.464	0.386	0.01081	1.692	2.47	3.205
δ_{10}	2.072	0.329	0.006066	1.461	2.065	2.733
δ_{11}	1.136	0.2781	0.006461	0.5982	1.134	1.679
δ_{12}	1.591	0.2812	0.00123	1.047	1.586	2.158
δ_{13}	1.337	0.2746	0.003862	0.796	1.339	1.871
δ_{14}	1.287	0.276	0.004606	0.748	1.287	1.818
δ_{15}	1.683	0.2876	0.00141	1.134	1.674	2.266
b_H	11.73	16.2	0.9232	2.433	7.48	63.51
a_H	18.69	25.87	1.475	3.871	11.85	102.9
σ	0.3059	0.04201	7.78×10^{-4}	0.2277	0.3044	0.3926
θ	0.126	0.3186	0.0113	2.13×10^{-5}	0.01097	0.9461

Table 4. Identification of the degradation rates for the 15 trajectories from the IRLED dataset.

| Trajectory	$\hat{\delta}_i$	$\hat{\theta}\hat{\beta}$	Rate Shape
1	1.19	1.97694	Bathtub
2	1.132	1.97694	Bathtub
3	1.076	1.97694	Bathtub
4	1.556	1.97694	Bathtub
5	1.603	1.97694	Bathtub
6	1.758	1.97694	Bathtub
7	1.629	1.97694	Bathtub
8	2.414	1.97694	Increasing
9	2.464	1.97694	Increasing
10	2.072	1.97694	Increasing
11	1.136	1.97694	Bathtub
12	1.591	1.97694	Bathtub
13	1.337	1.97694	Bathtub
14	1.287	1.97694	Bathtub
15	1.683	1.97694	Bathtub
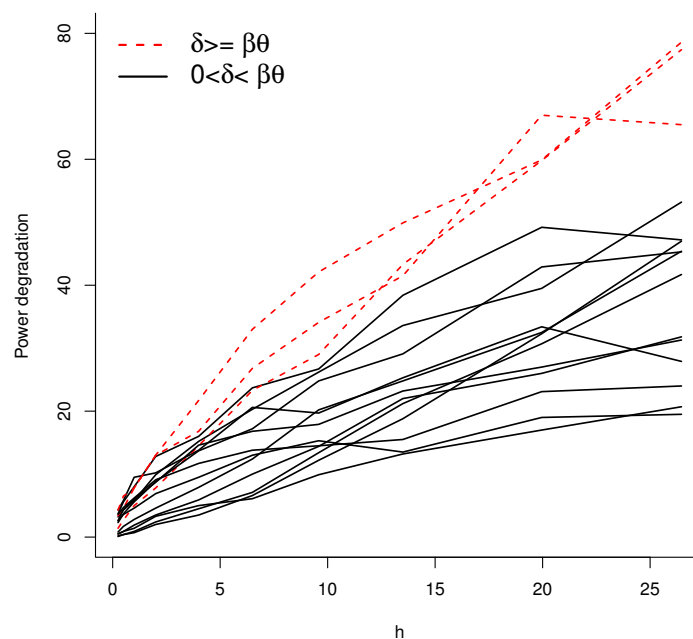
Figure 6. Illustration of the individual characterization for the IRLED dataset.

As in the previous case study, we also obtained the reliability function with $\omega = 90$ for the WP with a Hjorth rate and random effects for the IRLED dataset; this can be seen in Figure 7 as a continuous black line. Furthermore, we also fitted the CDWP in (2) to this dataset; the obtained parameters were $\hat{\mu} = 1.584$ and $\hat{\sigma} = 0.2375$. Based on these parameters, we also calculated the reliability for the CDWP, which can also be seen in Figure 7 as a dashed black line. Similar differences can be noted in this case study to those in the crack propagation dataset. First, the reliability function from the WP with a Hjorth rate had a wider behavior, having a lower reliability from around 45 h to 60 h and greater reliability from 60 h to 80 h. Finally, the fitting of both models was assessed via the DIC discussed in the first case study. For the WP with a Hjorth rate, the DIC obtained was 645.5, while for the CDWP, it was 668.5. Once again, the best fitting model was the one proposed in this paper, as it had the lowest DIC value.
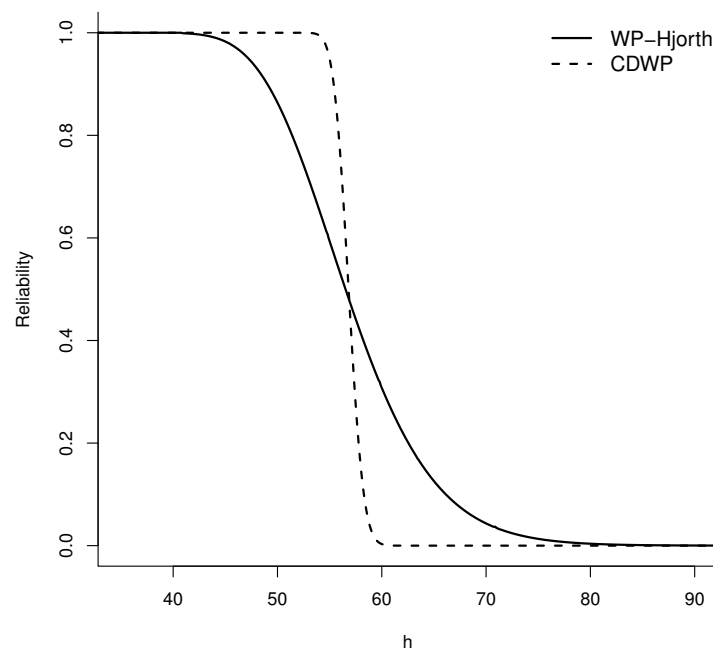

Figure 7. Estimated reliability values for the WP with a Hjorth rate and the CDWP for the IRLED dataset.

5. Concluding Remarks

This paper proposed an approach to integrate the Hjorth hazard rate function as the drift of the WP. As the drift of the WP defines a mean rate, it was possible to characterize the behavior of the degradation trajectories. This is an important addition, as the drift of the CDWP assumes a constant drift, which is not appropriate for most case studies since the degradation trajectories are random with uncertain behaviors due to the effect of multiple conditions. The proposed approach was complemented by considering a parameter of the Hjorth rate as random, to account for unit-to-unit variability. This random parameter allowed us to individually characterize the degradation rates for every trajectory. This consideration was reflected in the reliability estimation of a product. If a constant drift is assumed, then all of the degradation trajectories are assumed to have a constant growth, which would lead to an inaccurate reliability estimation. However, some trajectories at the beginning may have a low growth rate and then a larger growth rate, others may have a decreasing rate followed by an increasing rate, and some may have a constant rate. As the behavior of each trajectory is different, this is reflected in the reliability estimation, as the first-hitting times will vary in comparison with the scenario where all rates are assumed to be constant. These characteristics were illustrated by considering two degradation datasets. It can be noted that some degradation trajectories were identified to be exponentially increasing while others were identified to have a bathtub shape, as

presented in Figures 3a and 6. Indeed, these differences had an impact on the first-hitting times, as could be observed in the estimated reliability values in Figures 4 and 7, where the reliability for the CDWP was also obtained. First, from these figures, it was noted that the reliability for the WP–Hjorth model had a larger width, which was explained by the different identified degradation rates and their variation in the first-hitting times. Second, there was a crossing point for the reliability functions of both case studies at around $t = 30$ and $t = 60$, respectively.

The proposed approach can be extended in several aspects. Other parameters can be studied to introduce random effects, for example, the diffusion parameter σ to account for the variation within the increments in every degradation trajectory. This may be appropriate to further characterize the trajectories of products with trajectories that present a high variation either in their drift or diffusion. As for the Hjorth rate, β or θ can also be considered as simultaneous random effects. In this way, it may be possible to be more precise when identifying the rate for every trajectory. Furthermore, other hazard rate functions may be considered, for example, the ones that can also characterize an upside-down bathtub rate. However, these rates normally have complex forms that contribute to the complexity of the stochastic model and the estimation of its parameters.

Author Contributions: Conceptualization, L.A.R.-P.; methodology, L.A.R.-P.; software, L.A.R.-P.; validation, L.A.R.-P. and L.C.M.-G.; formal analysis, L.A.R.-P.; investigation, L.A.R.-P.; resources, L.A.R.-P., L.A.P.-D. and H.E.T.-P.; writing—original draft preparation, L.A.R.-P.; writing—review and editing, L.A.R-P., L.C.M.-G., L.A.P.-D. and H.E.T.-P.; visualization, L.C.M.-G., L.A.P.-D. and H.E.T.-P.; funding acquisition, L.A.R.-P., L.C.M.-G., L.A.P.-D. and H.E.T.-P. All authors have read and agreed to the published version of the manuscript.

Data Availability Statement: The original contributions presented in the study are included in the article, further inquiries can be directed to the corresponding author.

Conflicts of Interest: The authors declare no conflicts of interest.

References

1. Niu, H.; Zeng, J.; Shi, H.; Zhang, X.; Liang, J. Degradation modeling and remaining useful life prediction for a multi-component system with stochastic dependence. *Comput. Ind. Eng.* **2023**, *175*, 108889. [CrossRef]
2. Xie, G.; Li, X.; Peng, X.; Qian, F.; Hei, X. Estimating the Probability Density Function of Remaining Useful Life for Wiener Degradation Process with Uncertain Parameters. *Int. J. Control Autom. Syst.* **2019**, *17*, 2734–2745. [CrossRef]
3. Sung, S.I. Strategic Approaches for Assessing the Reliability Information during Product Development: Perspective of the Partially Accelerated Degradation Test. *Appl. Sci.* **2023**, *13*, 5448. [CrossRef]
4. Liu, L.; Li, X.; Sun, F.; Wang, N. A General Accelerated Degradation Model Based on the Wiener Process. *Materials* **2016**, *9*, 981. [CrossRef]
5. Hove, H.; Mlambo, F. On Wiener Process Degradation Model for Product Reliability Assessment: A Simulation Study. *Model. Simul. Eng.* **2022**, *2022*, 7079532. [CrossRef]
6. Whitmore, G.A. Estimating degradation by a wiener diffusion process subject to measurement error. *Lifetime Data Anal.* **1995**, *1*, 307–319. [CrossRef]
7. Pan, D.; Lu, S.; Liu, Y.; Yang, W.; Liu, J.B. Degradation Data Analysis Using a Wiener Degradation Model With Three-Source Uncertainties. *IEEE Access* **2019**, *7*, 37896–37907. [CrossRef]
8. Wang, X.; Wang, B.X.; Jiang, P.H.; Hong, Y. Accurate reliability inference based on Wiener process with random effects for degradation data. *Reliab. Eng. Syst. Saf.* **2020**, *193*, 106631. [CrossRef]
9. Zhou, S.; Tang, Y.; Xu, A. A generalized Wiener process with dependent degradation rate and volatility and time-varying mean-to-variance ratio. *Reliab. Eng. Syst. Saf.* **2021**, *216*, 107895. [CrossRef]
10. Jiang, P. Statistical Inference of Wiener Constant-Stress Accelerated Degradation Model with Random Effects. *Mathematics* **2022**, *10*, 2863. [CrossRef]
11. Xu, X.; Tang, S.; Yu, C.; Xie, J.; Han, X.; Ouyang, M. Remaining Useful Life Prediction of Lithium-ion Batteries Based on Wiener Process Under Time-Varying Temperature Condition. *Reliab. Eng. Syst. Saf.* **2021**, *214*, 107675. [CrossRef]
12. Guan, Q.; Tang, Y.; Xu, A. Objective Bayesian analysis for competing risks model with Wiener degradation phenomena and catastrophic failures. *Appl. Math. Model.* **2019**, *74*, 422–440. [CrossRef]
13. Wang, X.; Wang, B.; Niu, Y.; He, Z. Reliability Modeling of Products with Self-Recovery Features for Competing Failure Processes in Whole Life Cycle. *Appl. Sci.* **2023**, *13*, 4800. [CrossRef]

14. Zhang, Z.; Hu, C.; Si, X.; Zhang, J.; Shi, Q. A prognostic approach for systems subject to wiener degradation process with cumulative-type random shocks. In Proceedings of the 2017 6th Data Driven Control and Learning Systems (DDCLS), Chongqing, China, 26–27 May 2017; pp. 694–698. [CrossRef]

15. Zhang, J.; Si, X.; Du, D.; Hu, C.; Hu, C. Lifetime Estimation for Multi-Phase Deteriorating Process with Random Abrupt Jumps. *Sensors* **2019**, *19*, 1472. [CrossRef]

16. Sun, F.; Li, H.; Cheng, Y.; Liao, H. Reliability analysis for a system experiencing dependent degradation processes and random shocks based on a nonlinear Wiener process model. *Reliab. Eng. Syst. Saf.* **2021**, *215*, 107906. [CrossRef]

17. Palayangoda, L.K.; Butler, R.W.; Ng, H.K.T.; Yang, F.; Tsui, K.L. Evaluation of mean-time-to-failure based on nonlinear degradation data with applications. *IISE Trans.* **2021**, *54*, 286–302. [CrossRef]

18. Liu, H.; Huang, J.; Guan, Y.; Sun, L. Accelerated Degradation Model of Nonlinear Wiener Process Based on Fixed Time Index. *Mathematics* **2019**, *7*, 416. [CrossRef]

19. Lin, J.; Liao, G.; Chen, M.; Yin, H. Two-phase degradation modeling and remaining useful life prediction using nonlinear wiener process. *Comput. Ind. Eng.* **2021**, *160*, 107533. [CrossRef]

20. Wang, X.; Su, X.; Wang, J. Nonlinear Doubly Wiener Constant-Stress Accelerated Degradation Model Based on Uncertainties and Acceleration Factor Constant Principle. *Appl. Sci.* **2021**, *11*, 8968. [CrossRef]

21. Lyu, Y.; Zhang, Y.; Chen, K.; Chen, C.; Zeng, X. Optimal Multi-Objective Burn-In Policy Based on Time-Transformed Wiener Degradation Process. *IEEE Access* **2019**, *7*, 73529–73539. [CrossRef]

22. Giorgio, M.; Pulcini, G. A new age- and state-dependent degradation process with possibly negative increments. *Qual. Reliab. Eng. Int.* **2019**, *35*, 1476–1501. [CrossRef]

23. Giorgio, M.; Postiglione, F.; Pulcini, G. Bayesian estimation and prediction for the transformed Wiener degradation process. *Appl. Stoch. Model. Bus. Ind.* **2020**, *36*, 660–678. [CrossRef]

24. Muhammad, I.; Wang, X.; Li, C.; Yan, M.; Mukhtar, M.; Muhammad, M. Reliability Analysis with Wiener-Transmuted Truncated Normal Degradation Model for Linear and Non-Negative Degradation Data. *Symmetry* **2022**, *14*, 353. [CrossRef]

25. Xu, X.; Yu, C.; Tang, S.; Sun, X.; Si, X.; Wu, L. Remaining Useful Life Prediction of Lithium-Ion Batteries Based on Wiener Processes with Considering the Relaxation Effect. *Energies* **2019**, *12*, 1685. [CrossRef]

26. Xu, X.; Yu, C.; Tang, S.; Sun, X.; Si, X.; Wu, L. State-of-Health Estimation for Lithium-Ion Batteries Based on Wiener Process With Modeling the Relaxation Effect. *IEEE Access* **2019**, *7*, 105186–105201. [CrossRef]

27. Peng, W.; Li, Y.F.; Yang, Y.J.; Mi, J.; Huang, H.Z. Bayesian Degradation Analysis With Inverse Gaussian Process Models Under Time-Varying Degradation Rates. *IEEE Trans. Reliab.* **2017**, *66*, 84–96. [CrossRef]

28. Rodríguez-Picón, L.A.; Méndez-González, L.C.; Pérez-Olguín, I.J.C.; Hernández-Hernández, J.I. A study of the Inverse Gaussian Process with hazard rate functions-based drifts applied to degradation modelling. *Eksploat. Niezawodn. Maint. Reliab.* **2022**, *24*, 590–602. [CrossRef]

29. Giorgio, M.; Piscopo, A.; Pulcini, G. A new Wiener process with bathtub-shaped degradation rate in the presence of random effects. *Appl. Stoch. Model. Bus. Ind.* **2023**, *40*, 574–597. [CrossRef]

30. Hjorth, U. A Reliability Distribution with Increasing, Decreasing, Constant and Bathtub-Shaped Failure Rates. *Technometrics* **1980**, *22*, 99. [CrossRef]

31. Wu, W.; Ni, C. A study of stochastic fatigue crack growth modeling through experimental data. *Probabilistic Eng. Mech.* **2003**, *18*, 107–118. [CrossRef]

32. Konishi, S.; Kitagawa, G. *Information Criteria and Statistical Modeling*; Springer Science & Business Media: Berlin/Heidelberg, Germany, 2008.

33. Yang, G. *Life Cycle Reliability Engineering*; Wiley: Hoboken, NJ, USA, 2007. [CrossRef]